Structural Novelties in Anionic Cluster Halide Phases. Discrete Tetrahedral A_4Br^{+} Ions in Two New Zirconium Bromide Structures (A = Na−Cs)

Ru-Yi Qi and John D. Corbett*

Department of Chemistry, Iowa State University, Ames, Iowa 50011

Received July 2, 1997[⊗]

Suitable reactions of ABr, Zr, $ZrBr_4$, and an interstitial Z element in Ta containers at 850 °C afford two series of quaternary cluster phases containing A_4Br^{3+} ions. Cubic $(A_4Br)_2Zr_6(Z)Br_{18}$ phases occur for various combinations of A = Na−Cs, Z = Be, B, H, Mn. The combination with A = K, Z = B was structurally characterized (inverse fluorite, $Fm\bar{3}m$, $Z = 4$, $a = 16.191(2)$ Å). The 15-e cluster exhibits the appropriate magnetic moment, and this decreases toward the diamagnetic 14-electron limit in products with potassium deficiencies, $(K_{4-x})_2Zr_6Br_{18}B$, $x \leq \sim 0.5$. The tetragonal $Cs_4Br[Zr_6(B)Br_{12}]Br_4$ ($P\bar{4}2_1m$, $Z = 2$, $a = 12.5482(7)$ Å, $c = 11.5610(9)$ Å) contains a new type of puckered M_6Br_{16} layers with Cs_4Br^{3+} in tunnels normal to the layers. Both examples of A_4Br^{3+} ions have short central Br−A bonds plus three to nine more distant bromines in neighboring clusters about each A, respectively.

Introduction

The basic principles regarding the bonding within and around M_6X_{12}-type clusters appear to be well-established.[1,2] All 12 edges of the nominal octahedral metal core are always edge-bridged by halogen X^i (unless cluster condensation pertains). Furthermore, a halogen is always bound exo at each metal vertex, X^a. The latter may have three different functionalities, solely terminal X^a, intercluster bridging X^{a-a} or, with lower X/M ratios, a bifunctional role X^{a-i} (and the complementary X^{i-a}). Examples are known with 0−6 extra halides in some X^a role, this series leading to a continuous opening up of the intercluster bridge bonding until isolated $(M_6X_{12})X^a_6$ units are achieved. (A few cases of X^{i-i} as well as triply bridging X^{i-a-a}, etc., types are also known in halogen-poorer situations.) For discrete clusters of the earlier group 3 and 4 transition metals, there is an additional and powerful means to induce variations, the evident requirement of an interstitial atom Z within each cluster for stability, this atom contributing both additional electrons and central bonding. The selection of interstitial atoms and X/M proportions thus affords many opportunities to "force" the formation of certain interbridged cluster networks (or isolated examples) and, with electron-poorer Z or more X, the need for extra cations and their electrons in order to achieve favorable cluster-based electron counts, optimally 14 with main group Z. This electronic condition applies best with zirconium chlorides and less well to rare-earth-metal iodides[3] (where chloride examples are relatively sparse).

Other components of phase stability for these compounds appear to be efficacious space-filling structural arrangements and the obvious Coulombic contributions, the latter meaning that any countercations are preferentially surrounded by the more basic or negatively charged X^{a-a} and X^a atoms. Halogen atoms that are free and unbound to the cluster metal have heretofore been unknown.

The influence of all of these factors on the structure of a great many quaternary examples have led to some rather unusual features. The network and packing demands appear paramount, while the cations, particularly the larger alkali-metal members, seem to exert lesser influence on the structure and their environments. These factors may lead to examples of cations bound in some combination of low-coordination, asymmetric, oversized or otherwise inferior and often fractionally occupied sites, all of which naturally lead to unusual cation displacement parameters on X-ray refinement. Relevant and fairly extreme examples appear in $CsKZr_6Cl_{15}B$,[4] $Rb_5Zr_6Cl_{18}B$,[5] $Cs_3Zr_6Br_{15}C$,[6] $Rb_5Zr_6Br_{15}Be$,[7] and $KPr_6I_{10}Os$.[8]

The "fit" of many compounds in a given structure type is evidently so close that they often do not survive even a simple change in halogen. Our recent explorations of the bromides of rare-earth metals and zirconium have accordingly revealed several structure types that are presently unique to bromide,[9] including the advent of a variety of oligomeric $R_{16}Br_{20}Z_4$ clusters (R = Y, Sc).[10,11] We report here what in hindsight seems eminently plausible, two new crystalline arrangements that generate (contain) precisely the right cavity dimensions for an extra bromide to be bound in an A_4Br^{3+} ion. This larger unit in effect replaces what are normally rather poorly bound countercations that more or less line channels in quaternary cluster or network arrays, e.g., in $Rb_5Zr_6Br_{15}Be$.[7] The extra ABr component here presumably serves both to reduce the repulsion between the simple cations replaced and to improve their often inferior bonding to bromide on the walls of the cluster network. The previous absence of such extra, cluster-free halides once led to the reasonable conclusion that these must instead serve to open up any intercluster halogen bridges, viz., $Zr_6-Br^{a-a}-Zr_6 + Br^- \rightarrow 2Zr_6Br^a$, where Zr_6 refers to one vertex of some octahedral cluster. A few particular structural arrangements are already known that allow the simultaneous presence

[⊗] Abstract published in *Advance ACS Abstracts,* December 1, 1997.

(1) Corbett, J. D. In *Modern Perspectives in Inorganic Crystal Chemistry*; Parthé, E., Ed.; NATO ASI Series C; Kluwer Academic Publishers: Dordrecht, The Netherlands, 1992; pp 27−56.
(2) Corbett, J. D. *J. Alloys Compd.* **1995**, *229*, 10.
(3) Payne, M. W.; Corbett, J. D. *Inorg.Chem.* **1990**, *29*, 2246.
(4) Ziebarth, R. P.; Corbett, J. D. *J. Am. Chem. Soc.* **1987**, *109*, 4844.
(5) Ziebarth, R. P.; Corbett, J. D. *J. Am. Chem. Soc.* **1989**, *111*, 3272.
(6) Qi, R.-Y.; Corbett, J. D. *Inorg. Chem.* **1995**, *34*, 1657.
(7) Qi, R.-Y.; Corbett, J. D. *Inorg. Chem.* **1995**, *34*, 1646.
(8) Lulei, M.; Corbett, J. D. *Z. Anorg. Allg. Chem.* **1996**, *622*, 1677.
(9) Qi, R.-Y.; Corbett, J. D. *J. Solid State Chem.*, submitted for publication.
(10) Steinwand, S. J.; Corbett, J. D. *Inorg. Chem.* **1996**, *35*, 7056.
(11) Steinwand, S. J.; Corbett, J. D.; Martin, J. D. *Inorg. Chem.*, in press.

S0020-1669(97)00818-5 CCC: $14.00

Table 1. Lattice Constants of Compounds with $(K_4Br)_2Zr_6Br_{18}B$-Type Structures ($Fm\bar{3}m$, 22 °C)

	a (Å)	*V* (Å^3)	estd yield (%)
A, Z in $(A_4Br)_2Zr_6Br_{18}Z$[a]			
K, B[b]	16.197(1)	4248.8(9)	>95
K, Be	16.240(2)	4283(1)	95
K, H	16.178(1)	4234(1)	90
K, Mn[c]	16.320(2)	4347(1)	50
Rb, B	16.585(2)	4562(2)	>90
Rb, Be	16.628(1)	4597.6(8)	>90
Rb, Mn[c]	16.692(3)	4651(3)	50
Na, B	15.704(3)	3873(2)	>95
loaded composition			
$(K_4Br)_2Zr_6Br_{18}B$	16.196(1)	4248.5(9)	>90
$(K_{3.75}Br)_2Zr_6Br_{18}B$	16.201(1)	4252.5(8)	>90
$(K_{3.5}Br)_2Zr_6Br_{18}B$	16.209(2)	4259(2)	90
KZr_6Br_9B[d]	16.191(2)	4244(2)	10−15
$K_4Zr_6Br_{15}B$	16.2025(7)	4253.5(5)	50

[a] Compounds obtained from stoichiometric reactions at 830−850 °C unless noted. [b] 10% excess Zr. [c] 20−30% excess Mn, which reduced the yield through the formation of byproduct $ZrMn_2$. [d] Source of data crystal.

of halide functionalities that are not adjacent in terms of basicity or the number of bonded metal neighbors.[12,13]

Experimental Section

The metal source, the production of 100-mesh powdered Zr, the synthesis and purification of $ZrBr_4$, the handling of reactants and products in gloveboxes, the reaction techniques in welded Ta containers, and the characterization means have been described before. Likewise, Guinier powder diffraction was used for precise lattice parameter determinations, phase identification, and yield estimates.[6,7] The B and Be used were stated to be 5−9's and 3−9's, respectively (Aldrich). Reagent grade sodium, potassium, and rubidium bromides were first vacuum sublimed. The Mn chips (4−9's) came from Johnson-Matthey.

Syntheses. The very dark purple $(K_4Br)_2Zr_6Br_{18}B$ was first observed after a reaction targeted on a hypothetical cluster phase KZr_6Br_9B that had been carried out for 3 weeks at 850 °C. According to the powder pattern, ∼10−15% of an unknown phase was present in addition to a major amount of $Zr_6Br_{14}B$ (stuffed Nb_6Cl_{14}[14]). The same new phase was subsequently obtained in about 25 and 50% yields from reactions loaded as $K_2Zr_6Br_{10}B$ and $K_4Zr_6Br_{15}B$, respectively. The new Guinier powder pattern contained fewer lines than do most other phases, possibly indicating a high lattice symmetry. After the crystal structure and thence the composition of this phase had been determined, a stoichiometric reaction produced it in about 90% yield. Several other examples of new compounds with the same structure type were prepared utilizing various combinations of Na, K, or Rb as countercations and H, Be, B, or Mn as interstitials. Their yields and lattice dimensions are given in Table 1. The assigned compositions are based on the quantitative correspondence of the individual powder patterns to those calculated on the basis of the new structure and the high yields from stoichiometric reactions. A phase with this structure does not form with Cs^+ as the countercation, while a similar yet distinctive powder pattern was observed when Na and Be were loaded. The splitting of some of the lines in the last as well as some weak extra lines suggest a phase with a probably related but lower symmetry structure is formed.

Since the stoichiometric $(K_4Br)_2Zr_6Br_{18}B$ contains a 15-electron cluster, variations of the reaction composition were pursued in parallel with magnetic susceptibility studies to see whether a nonstoichiometry existed. Lattice constants from reactions run in this exploration are listed in the lower part of Table 1. Dimensional changes testifying to compositional variations are quite small, but magnetic data indicate significant electronic variations are achieved (see Results and Discussion).

$(Cs_4Br)Zr_6Br_{16}B$ was first seen as the major product of a reaction loaded with a $Cs_2Zr_6Br_9B$ stoichiometry and run at 830 °C for 30 days. This phase was not obtained from a reaction with a composition $CsZr_6Br_9B$, rather $Cs_{3.4}Zr_6Br_{15}B$[6] was, so the new compound had to contain more cesium than the latter. Thus, another reaction loaded as $Cs_4Zr_6Br_{15}B$ produced about 90% of the dark purple phase sought. However, well-grown crystals were obtained from yet another reaction with the stoichiometry $Cs_8Zr_6Br_{20}B$ that was aimed at the synthesis of the cesium analogue of the above cubic potassium phase. The excess CsBr or, more likely, Cs_2ZrBr_6 probably served as a useful flux for crystal growth.

Structure Determinations. For $(K_4Br)_2Zr_6Br_{18}B$, oscillation plus zero and first layer Weissenberg photographs of a needlelike crystal from the KZr_6Br_9B composition (a) established that the crystal selected was single and not that of the orthorhombic $KZr_6Br_{14}B$ co-product and (b) showed the body-centered tetragonal equivalent of the correct face-centered cubic cell.

Reflection data for one octant collected on a Rigaku AFC6R diffractometer at room temperature were corrected for absorption by means of one ψ-scan. The data were consistent with $m3m$ Laue symmetry, and the highest symmetry space group among the three possibilities, $Fm\bar{3}m$, was proven to be correct by subsequent refinements. Direct methods (SHELXS-86[15]) provided the correct model. Peak assignments were somewhat ambiguous because of the similar scattering powers of Br and Zr, but a drawing made with the initial position set enabled these to be clearly distinguished as belonging to a $Zr_6Br_{12}Br_6$ cluster unit. The supposed K locations were established with the aid of a difference Fourier map after isotropic refinement of the heavy atom positions in the cluster by TEXSAN.[16] One of the two sites so found was not connected to any heavy atom, and the peak (∼30 e$^-$/Å^3) was too large for a K atom. Assignment of it as a Br atom gave reasonable distances to a tetrahedron of surrounding K atoms that defined the polycation $[K_4Br]^{3+}$.

Isotropic refinement of all atoms converged at $R(F) = 9.1\%$ and $R_w = 4.7\%$, and the anisotropic refinements smoothly converged at $R = 4.7\%$ and $R_w = 2.2\%$. However, this left the interstitial B with a negative thermal parameter. This was supposed to result from a insufficient absorption correction (one ψ-scan) for the needlelike crystal with ∼1:1:9 relative dimensions ($\mu = 208.5$ cm^{-1}). Therefore, a cylindrical correction provided by the program PABSN[17] was applied. Least-squares refinement with the data so prepared produced a small positive temperature factor for interstitial boron and a convergence with distinctly smaller residuals and errors ($R = 3.2\%$ and $R_w = 1.6\%$). Variation of the occupancy of the single type of K^+ yielded 100(1)% after refinement of the secondary extinction coefficient and the isotropic thermal parameter of boron. The composition of the phase is accordingly $K_8Zr_6Br_{20}B$, which means a 15-e$^-$ count for the Zr_6 skeleton.

Refinement of a second single crystal from a K-limited reaction loaded as $K_4Zr_6Br_{15}B$ (Table 1) was also performed. Refinement of the occupancy of K^+ near the end gave 86(1)%, meaning a $(K_{3.44(4)}Br)_2Zr_6Br_{18}B$ composition and a nominal 13.9(1)-e$^-$ cluster phase. It is interesting to notice that the phase with the higher K content (above) came from the reaction with less $K/Zr_6Br_{20}B$, in the loaded stoichiometry. In fact, a more reduced system, with ∼40% unreacted Zr, appears crucial to the formation of the former stoichiometric compound with a 15-e cluster. The same phenomenon has been observed in some chloride systems.[18,19]

For $(Cs_4Br)Zr_6Br_{16}B$, data collection was done at room temperature with the aid of an ENRAF NONIUS CAD4 diffractometer. Orientation analysis indicated a primitive tetragonal cell, and two octants of data were collected with an $\omega-\theta$ scan mode. The only absence condition observed was $0k0$ for $k = 2n + 1$, giving only two possible space groups $P\bar{4}2_1m$ (No. 113) and $P4_12$ (No. 90), both acentric. The former

(12) Köckerling, M.; Qi, R.-Y.; Corbett, J. D. *Inorg. Chem.* **1996**, *35*, 1437.
(13) Park, Y.; Corbett, J. D. *Inorg. Chem.* **1994**, *33*, 1705.
(14) Simon, A.; von Schnering, H.-G.; Wöhrle, H.; Schäfer, H. *Z. Anorg. Allg. Chem.* **1965**, *339*, 155.
(15) Sheldrick, G. M. *SHELXS-86*, Programs for Structure Determination; Universität Göttingen: Göttingen, Germany, 1986.
(16) *TEXSAN*, version 6.0 package; Molecular Structure Corp.: The Woodlands, TX, 1990.
(17) Karcher, B. A. Ph.D. Dissertation, Iowa State University, Ames, IA, 1981.
(18) Ziebarth, R. P.; Corbett, J. D. *Inorg. Chem.* **1989**, *28*, 626.
(19) Zhang, J.; Ziebarth, R. P.; Corbett, J. D. *Inorg. Chem.* **1992**, *31*, 614.

Table 2. Selected Crystal Data

composition	$(K_4Br)_2Zr_6Br_{18}B$	$(Cs_4Br)Zr_6Br_{16}B$
fw	2469.0	2448.1
cryst syst	cubic	tetragonal
space group	$Fm\bar{3}m$ (No. 225)	$P\bar{4}2_1m$ (No. 113)
cell params[a]		
a (Å)	16.191(2)	12.5482(7)
c (Å)		11.5610(9)
V (Å^3)	4244(2)	1820.4(2)
Z	4	2
density, calc (g cm^{-3})	3.86	4.47
μ(Mo Kα) (cm^{-1})	208.5	240.4
R^b (%)	3.2	4.3
$R_w{}^b$ (%)	1.6	3.2

[a] Cell data from Guinier X-ray powder patterns with Si as internal standard, $\lambda = 1.540\,562$ Å, 22 °C. [b] $R = \sum||F_o| - |F_c||/\sum|F_o|$; $R_w = [\sum w(|F_o| - |F_c|)^2/\sum w(F_o)^2]^{1/2}$; $w = \sigma_F^{-2}$.

was tried first, and its correctness was later proven by a successful refinement. An empirical absorption correction applied according to three averaged ψ-scans yielded $R_{av} = 4.2\%$ for $I > 3\sigma_I$. The initial model was again obtained by direct methods, which provided the correct positions of all atoms. The isotropic refinement converged to $R = 6.8\%$ and $R_w = 5.0\%$, and the anisotropic refinement smoothly converged at $R = 5.2\%$ and $R_w = 3.8\%$. The other enantiomer was taken to be the correct model since its refinement converged at $R = 4.3\%$, $R_w = 3.2\%$. The occupancy of the Cs position refined to 1.008(5). The interstitial boron lies in the (0, 1/2, z)-type position, and the refined z value, 0.178(8), deviates from the center of the cluster (0, $^1/_2$, 0.163) by only 2σ, which is taken to be insignificant.

Some refinement parameters for both structures are given in Table 2. Additional information on the data collections and refinements together with the anisotropic ellipsoidal parameters are given in the Supporting Information. These and the F_o/F_c listing are also available from J.D.C.

Magnetic Susceptibilities. These data were measured at 3 T between 6 and 300 K on a Quantum Design MPMS SQUID magnetometer. Tens of milligrams of weighed powder were held between silica rods in an apparatus of improved design.[20] The data were corrected for diamagnetism of both the container and the atom cores.

Result and Discussion

The new compounds $K_8Zr_6Br_{20}B$ (and its isotypes, Table 1) and $Cs_4Zr_6Br_{17}B$ all contain isolated bromine-centered A_4Br^{3+} tetrahedra that are relatively well-bound within cavities or tunnels in the anionic cluster array. The atomic positional and isotropic-equivalent ellipsoidal data for the two parent structures are listed in Table 3, and the important distances, in Tables 4 and 5, respectively.

$(K_4Br)_2Zr_6Br_{18}B$. The contents of the face-centered-cubic unit cell are illustrated in Figure l, where it can be seen that the ccp array of formal $Zr_6Br_{18}B^{6-}$ anions contain K_4Br^{3+} units in all tetrahedral cavities, i.e., in the hierarchical equivalent of the inverse fluorite structure. A similar Na_4Cl^{3+} unit is known in sodalite.[21] Roughly the same cluster arrangement has also been seen before in the structure of $Li_6Zr_6Cl_{18}H$, which occurs in a squashed rhombohedral lattice ($\alpha = 111.08°$).[19] There, the much smaller Li^+ occupy distorted octahedral sites defined by six chlorine atoms, half Cl^a and half Cl^i. Here, the designated K_4Br^{3+} units are in fact l2-bonded to the four anionic cluster neighbors in the manner shown in Figure 2. Thus the extra Br3 ($\bar{4}3m$ site symmetry) is four-bonded to K ions, and each of the latter ($3m$) is surrounded by an approximate tetrahedron of Br3 and three exo Br2^a atoms on three neighboring clusters, the distance to the more basic Br3 being 0.23 Å less than that to Br^a. The average d(K−Br), 3.23 Å, is 0.10 Å less than the sum of the crystal radii for Br (CN6) and K (CN4),[22] presumably because there are only four neighbors about Br3. Structurally, the isolated Br^- must reduce repulsions among positively charged K^+ countercations that otherwise would be bonded only to bromide on the clusters. The $Zr_6(B)Br_{12}Br_6$ cluster exhibits what might be viewed as somewhat tight Br1^i−Br2^a contacts about each vertex, 3.66 Å (Table 4). The fact that these are bound to two Zr, and one Zr and one K, respectively, should mean the effective closed-shell radii are less that those of an ideal bromide ion.

The structure of a less-reduced version was also refined to be $(K_{3.44(4)}Br)_2Zr_6Br_{18}B$, meaning a nominal l3.9(1)-electron cluster is present vs the 15-electron count in the above compound. The structural data for the oxidized version are not reported here since the metric differences are rather small; rather the composition vs magnetic results are more meaningful (below). The other versions of this structure type are assigned the nominal compositions of the parent structure in Table 1, although those with Z = B or Mn would be well-reduced and perhaps additional examples with somewhat cation-deficient $A_{4-x}Br$ units. Note that a 14-electron cluster also exists in the stoichiometric beryllide, and both the Be and B analogues occur with either Rb^+ or K^+ ions (Table 1).

Table 3. Positional and Isotropic-Equivalent Thermal Parameters for $(K_4Br)_2Zr_6Br_{18}B$ and $(Cs_4Br)Zr_6Br_{16}B$

atom	Wyckoff position	x	y	z	$B_{eq}{}^a$ (Å^2)
		$(K_4Br)_2Zr_6Br_{18}B$			
Zr	24e	0.1437(1)	0	0	1.47(6)
Br1	48h	0	0.16629(7)	y	2.39(4)
Br2	24e	0.3190(1)	0	0	3.16(7)
Br3	8c	$^1/_4$	$^1/_4$	$^1/_4$	3.319(1)
K[b]	32f	0.3591(2)	x	x	5.379(2)
B	4a	0	0	0	0.3(10)
		$(Cs_4Br)Zr_6Br_{16}B$			
Zr1	4e	0.4064(2)	$x + ^1/_2$	0.6951(3)	1.09(9)
Zr2	4e	0.4065(2)	$x + ^1/_2$	0.9811(3)	1.05(8)
Zr3	4e	0.1314(1)	$x + ^1/_2$	0.1595(4)	1.05(7)
Br1	2c	0	$^1/_2$	0.8301(6)	1.5(1)
Br2	4e	0.2946(2)	$x + ^1/_2$	0.1636(4)	1.66(8)
Br3	8f	0.2437(2)	0.0451(2)	0.6776(3)	1.8(1)
Br4	4e	0.2932(2)	$x + ^1/_2$	0.5254(3)	1.8(1)
Br5	2c	0	$^1/_2$	0.4929(6)	1.8(1)
Br6	8f	0.2418(2)	0.0409(2)	0.0005(3)	1.6(1)
Br7	4e	0.2881(2)	$x + ^1/_2$	0.8383(4)	1.56(8)
Br8	2b	0	0	$^1/_2$	3.2(2)
Cs	8f	0.2206(1)	0.0229(1)	0.3371(2)	3.31(9)
B	2c	0	$^1/_2$	0.178(8)	3(1)

[a] $B_{eq} = (8\pi^2/3)\sum_i\sum_j U_{ij}a_i{*}a_j{*}\vec{a}_i\vec{a}_j$.

Table 4. Important Bond Distances (Å) and Angles (deg) in $(K_4Br)_2Zr_6Br_{18}B$

Zr−Zr	×4	3.290(2)
Zr−B		2.326(2)
Zr−Br1^i	×4	2.717(1)
Zr−Br2^a		2.840(3)
K−Br3		3.061(5)
K−Br2^a	×3	3.290(4)
K−Br1^i	×6	3.889(1)
$\bar{d}$(CN = 4)		3.233
Br1−Br1^a	×4	3.808(1)
		3.834(2)
Br1−Br2	×2	3.655(2)
Br2−Zr−B		180.00
K−Br3−K	×4	109.47
Br2−K−Br3		133.35(8)
Br1−Zr−Br1	×2	164.60(5)

[a] d(Br−Br) < 4.0 Å.

(20) Guloy, A. M.; Corbett, J. D. *Inorg. Chem.* **1996**, *35*, 4669.
(21) Newnham, R. E. In *Structure-Property Relations*; Roy, R., Ed.; Springer-Verlag: New York, 1975; p 134.
(22) Shannon, R. P. *Acta Crystallogr.* **1976**, *A32*, 751.

Table 5. Important Bond Distances (Å) and Angles (deg) in $(Cs_4Br)Zr_6Br_{16}B$[a]

Zr1−Zr1		3.322(7)
Zr1−Zr2		3.306(4)
Zr1−Zr3	×2	3.320(4)
Zr2−Zr2		3.320(7)
Zr2−Zr3	×2	3.291(4)
$\bar{d}$		3.308
Zr1−B		2.22(6)
Zr2−B		2.47(7)
Zr3−B		2.341(9)
$\bar{d}$		2.34
Zr1−Br3[b]	×2	2.691(2)
Zr1−Br5		2.731(6)
Zr1−Br7		2.674(5)
Zr2−Br1		2.745(6)
Zr2−Br6	×2	2.677(3)
Zr2−Br7		2.670(5)
Zr3−Br3	×2	2.680(4)
Zr3−Br6	×2	2.691(5)
Zr1−Br4[a]		2.807(6)
Zr2−Br2[a−a]		2.897(6)
Zr3−Br2[a−a]		2.896(5)
Cs−Br8		3.360(2)
Cs−Br2[a−a]		3.619(4)
Cs−Br4[a]		3.725(4)
Cs−Br4[a]		3.749(4)
Cs−Br7[i]		3.900(4)
Cs−Br6[i]		3.908(4)
Cs−Br3[i]		3.955(4)
$\bar{d}$		3.745
Br1−Br2	×2	2.646(4)
Br2−Br3	×2	3.662(4)
Br2−Br6	×2	3.681(5)
Br3−Br4		3.670(4)
Br4−Br5		3.676(4)
Br4−Br7		3.619(6)
Br6−Br7		3.637(4)
Br3−Zr1−Br3		167.4(2)
Br1−Zr2−Br7		165.3(2)
Br6−Zr2−Br6		165.0(2)
Br3−Zr3−Br6		165.7(1)
Zr2−Br2−Zr3		132.3(2)
Zr1−Zr1−Zr2		90.0(1)
Zr1−Zr1−Zr3	×2	59.99(6)
Zr3−Zr1−Zr3	×2	89.2(1)
Zr2−Zr1−Zr3		59.6(1)
Cs−Br8−Cs	×2	111.85(9)
	×4	108.29(4)

[a] d(Cs−Br) < 4.0 Å; d(Br−Br) < 3.7 Å. [b] Br[i] functions.

The formation of the new structure as both the potassium and rubidium bromide borides affords a rather remarkable contrast to the composition and structure reported some time ago for $Rb_5Zr_6Cl_{18}B$ and its potassium analogue.[5] There, close-packed layers of isolated $Zr_6(B)Br_{18}^{5-}$ clusters are stacked in an eclipsed manner to generate three different high-coordination Rb (K) sites, one of which is rather asymmetric. The yield of this chloride was highest when the reactions were loaded slightly halide-deficient, while the precise $A_5Zr_6Cl_{18}B$ stoichiometries gave either Rb_2ZrCl_6 plus an unknown or $K_2Zr_6Cl_{15}B$. Formation of the zirconium(IV) product in both cases naturally leaves the remaining material deficient in halide (and A). Although reactions were not run with excess ACl, either the phase fields for comparable $(A_4Cl)_2Zr_6Cl_{18}B$ products are very small or neither analogous phase exists, perhaps because the chloride ion is of insufficient size to separate the four cations in the tetrahedral cluster adequately.

Examination of the new $K_8Zr_6Br_{20}B$ structure shows that the body-centered position and three equivalent sites on the midpoints of the cell edges are empty. These (octahedral) positions have six Br2 neighbors at 2.93 Å, suitable for Na^+ but probably not K^+, but their additional occupation would not be preferred electronically in the presence of what are already 15-electron boride clusters. Therefore, a reaction loaded as $(K_4Br)_2NaZr_6Br_{18}Be$ was run at 850 °C for 4 weeks. The powder pattern of the product fit that of the expected structure well and with a lattice constant 0.05 Å less than the all-potassium example. However, the magnetic susceptibility measurements showed none of the expected paramagnetism of a 15-electron cluster, only the rather common TIP-like behavior of 14-electron units. Evidently sodium only substituted in the potassium sites. However, this site may have been occupied in the product of a reaction aimed at the all-sodium $Na_8Zr_6Br_{20}Be$, which gave a powder pattern showing about 20% $Zr_6Br_{12}Be$[9] plus a potassium-like phase that showed some line splittings. The latter product should be sodium-richer according to the overall composition, possibly $(Na_4Br)_2NaZr_6Br_{20}Be$. Indexing with TREOR[23] gave a hexagonal (or trigonal) cell with $a = 18.07(1)$ Å, $c = 11.156(5)$ Å, and $Z = 3$. However, workable single crystals could not be found.

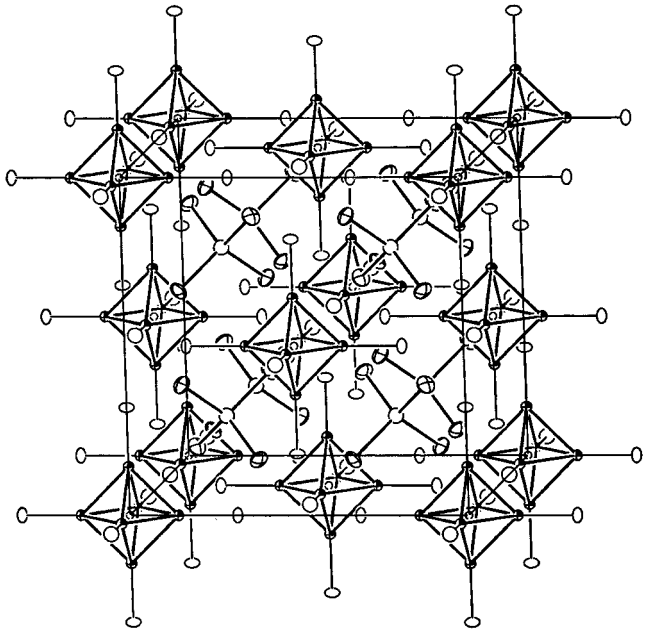

Figure 1. Cell contents of cubic $(K_4Br)_2Zr_6Br_{18}B$, with the edge-bridging Br[i] on each cluster omitted for clarity. The clusters define a face-centered cube with K_4Br^{3+} in tetrahedral cavities (70% probability ellipsoids; those for K atoms are crossed, and those for Zr, quarter-shaded).

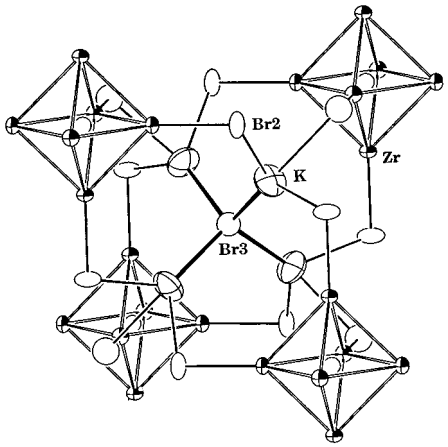

Figure 2. Details of the bonding of each potassium in K_4Br^{3+} to three Br[a] atoms each on four neighboring clusters (Br[i] omitted).

Magnetic Susceptibility Studies. The phase breadth of $(K_{4-x}Br)_2Zr_6Br_{18}B$ appears to be at least $0 \le x \le \sim 0.5$ (Table 1). The $x = 0$ limit corresponds to a 15-electron cluster with presumably one unpaired electron in an a_{2u} orbital. This situation appears to pertain to the product of a reaction loaded as $(K_4Br)_2Zr_6Br_{18}B$, plus 10% excess Zr from which came the data crystal. A moment of 1.623(1) μ_B was obtained from a nonlinear fit with $\theta = -23.2(4)$ K and TIP $= 1.211 \times 10^{-4}$ emu mol^{-1}, a typical value.[10,11] A value of 1.57(1) μ_B was likewise obtained from the product of a stoichiometric reaction ($a = 16.196(1)$ Å, Table 1) where a small potassium deficiency would probably occur. The moment continued to decrease when less potassium was incorporated in K_4Br^{3+}, as would be expected, 1.1(1) μ_B for the $(K_{3.75}Br)_2Zr_6Br_{18}B$ reaction and 0.78(6) μ_B with $(K_{3.5}Br)_2Zr_6Br_{18}B$. It is clear that the potassium contents achieved in these are evidently greater than what was loaded; note that a still K-poorer sample loaded as $K_4Zr_6Br_{15}B$ yielded (in part) the crystallographically refined product $(K_{3.44}Br)_2Zr_6Br_{18}B$. The last compound was unavailable phase-pure, but it should be substantially diamagnetic.

$(Cs_4Br)Zr_6Br_{16}B$. This phase is very rich in new structural features: (a) an extraordinary polycation $[Cs_4Br]^{3+}$ that both fills tunnels normal to the layers and is a little better isolated from the cluster cage than in the above potassium salt and (b) puckered or wavy layers of the first cis-interconnected 6−16 type clusters. As before, the "odd" Br8 atom centers a Cs_4 tetrahedron, in this case slightly distorted to $\bar{4}$ (S_4) symmetry with internal angles of 111.8 and 108.3°. The internal Cs−Br8 distance of 3.36 Å is somewhat more distinctive than was found for K_4Br^{3+}; the range of additional Cs−Br distances to the more numerous outer neighbors of Cs group as 3.62−3.75 Å to three Br^{a-a} and Br^a followed by ≥3.90 Å to six less basic edge-bridging Br^i (only half of which are listed in Table 5). The outer bromine neighbors are members of eight clusters about each Cs_4Br^{3+}, this number (rather than the four around K_4Br^+) originating with the linked array of clusters now present. The average of the seven shortest Cs−Br distances (Table 5) is 0.04 Å greater than the sum of crystal radii for CN6 Br^- and CN8 Cs^+,[22] but the range therein is large, 0.6 Å. The low coordination number of bromine is again presumably responsible for the unique 3.36 Å Cs−Br8 distance.

A snapshot of the new type of matrix that affords these unusual features is shown in Figure 3 in a view down the $\bar{4}$ axis of the tetragonal cell (from which all edge-bridging Br^i have been omitted for clarity). (The $\bar{4}$ axes lie along 0,0,*z* and $^1/_2,^1/_2,z$, with 2-fold axes along these and $0,^1/_2,z$, etc., and mirror planes along $(x,^1/_2 - x,z)$. Each of the relatively ordinary C_{2v} clusters is bridged at four vertices (via $Bi2^{a-a}$) to like clusters, while two cis-vertices are bonded only to terminal $Br4^a$ atoms. A shorthand description of the composition is $Zr_6(B)(Br^i)_{12}(Br^{a-a})_{4/2}(Br^a)_2$. Figure 4 is an extended [001] view that better shows how the bridging Br2 atoms link the clusters into layers, which are stacked in an eclipsed manner with no interconnections. Figure 5 normal to $\bar{c}$ makes clearer how the layers previously seen in projection are puckered via bridging Br^{a-a} atoms at four adjacent vertices while the two exo $Br4^a$ in cis-positions (and Br^{a-a}) line what are cation cavities between them. The closest approach of Cs_4Br^{3+} cations, 8.87 Å, is in the tunnels along [110] and [1$\bar{1}$0] directions between the layers (diagonally in the plane of the page in Figure 4). The tunnels normal to the layers that are evident in the earlier figures contain polycations clusters separated by 11.56 Å (*c*). Clearly, the stability of the Cs_4Br^+ cations in this structure, and vice versa, derives from the close match of these new units to the new network arrangement and, of course, to the charge.

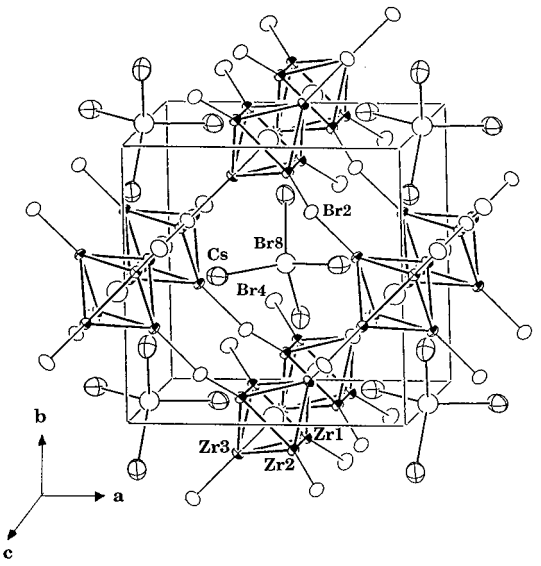

Figure 3. ~[001] view of the tetragonal unit cell contents in $(Cs_4Br)Zr_6Br_{16}B$ with cluster-bridging Br2 and terminal Br4 included, but without Br^i atoms. The view shows two puckered layers of bridged clusters in projection with Cs_4Br^{3+} between them. (80% probability ellipsoids are shown with those of Cs crossed and those of Zr quarter-shaded.)

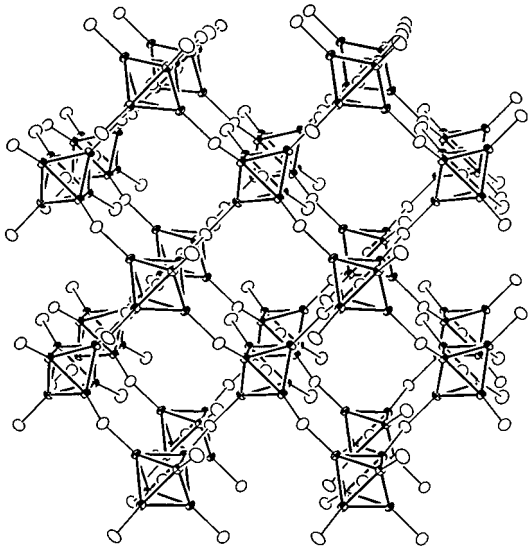

Figure 4. Larger [001] view of the puckered layers of clusters generated by bridging Br^{a-a}, with terminal Br^a projecting more into the interlayer region. The two eclipsed layers shown are not directly interconnected. Cs_4Br^{3+} cations lie between these in the square cavities (70%).

The first examples reported for this M_6X_{16}-type stoichiometry, orthorhombic $Na_4Zr_6Cl_{16}Be$ and monoclinic $Cs_3Zr_6Cl_{16}C$,[18] exhibit basically planar layers of interbridged clusters with the two trans-Zr−Cl^a functions directed outward and toward the interlayer cation sites. Small to moderate tilting of neighboring clusters from normals to the layers and a staggered stacking of these appear to afford improved accommodation of cations of different numbers and sizes. We have subsequently refined $Na_3Zr_6Br_{16}B$ and $Cs_4Zr_6Br_{16}Be$ as isostructural with the foregoing, respectively, save for different occupancies of cation sites, the latter compound now containing an ideal 14-electron cluster.[9]

The discovery of the new compounds described herein again emphasizes the striking range of compositions and structures

(23) Werner, P. E. *TREOR-V5*; Department of Structure Chemistry, Arrhenius Laboratory, University of Stockholm: Stockholm, Sweden, 1984.

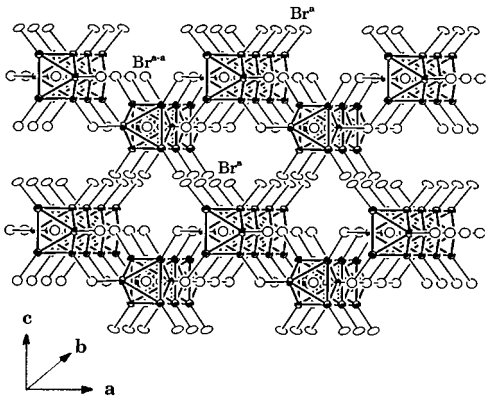

Figure 5. View normal to $\vec{c}$ (vertical) of two puckered and nested layers of linked $Zr_6Br_{16}B^{3-}$ clusters in $(Cs_4Br)Zr_6Br_{16}B$. Note that the array of cavities between them lined by Br^{a-a} and cis-Br^a are the Cs_4Br^{3+} cation sites. The vertical cluster displacements are 3.32 Å (90%).

that can be generated with the synthetic variables available. All of these appear to depend vitally on space-filling efficiencies of the cluster networks and their halides and, usually, some necessary countercations. The appearance of compounds containing these novel A_4Br^{3+} species once again surprises us with the unexpected, even unimagined, versatility that is possible.

Acknowledgment. The authors are indebted to Jerome Ostenson for the magnetic data. This research was supported by the National Science Foundation, Solid State Chemistry, through Grants DMR-9207361 and -9510278 and was carried out in the facilities of the Ames Laboratory, U.S. Department of Energy.

Supporting Information Available: Tables giving the details of data collection and refinement conditions and results plus anistropic displacement parameters for both structures (2 pages). Ordering information is given on any current masthead page.

IC970818U